Colloids and Surfaces B: Biointerfaces 148 (2016) 518–525

Contents lists available at ScienceDirect

Colloids and Surfaces B: Biointerfaces

journal homepage: www.elsevier.com/locate/colsurfb

Redox responsive liposomal nanohybrid cerasomes for intracellular drug delivery

Gaoxin Zhou[a,b], Lushen Li[a,b,e], Jing Xing[a,b], Shivakumar Jalde[a,b], Yan Li[a,b], Jin Cai[c], Junqing Chen[c], Peidang Liu[d], Ning Gu[a,b,*], Min Ji[a,b,*]

[a] School of Biological Science & Medical Engineering, Southeast University, Nanjing 210096, China
[b] School of Biological Science and Medical Engineering & Collaborative Innovation Center of Suzhou Nano Science and Technology, Southeast University, Suzhou 215123, China
[c] School of Chemistry & Chemical Engineering, Southeast University, Nanjing 210096, China
[d] School of Medicine, Southeast University, Nanjing 210009, China
[e] The Center for Vascular and Inflammatory Diseases, University of Maryland, Baltimore, MD 21201, U.S.A, USA

ARTICLE INFO

Article history:
Received 10 May 2016
Received in revised form 29 August 2016
Accepted 23 September 2016
Available online 23 September 2016

Keywords:
Cerasome
Redox responsive
Doxorubicin
Morphological stability

ABSTRACT

Cerasome is a freshly developped bilayer vehicle that resemble traditional liposome but has higher mophorlogical stability. In this study, a novel redox-responsive cerasome (RRC) was developed for tumor-targeting drug delivery. The cerasome-forming lipid (CFL) that comprise a cleavable disulfide bond as connector unit of the triethoxysilyl head and the hydrophobic alkyl double chain was synthesized and subsequently used to prepare cerasome through ethanol injection method. RRC that has liposome-resembling lipid bilayer structure was proved being outstanding at drug loading capacity as well as morphological stability as compared to conventional liposomes. In addition, *in vitro* drug release tests of DOX/RRCs showed a redox-responsive drug release profile: accelerated DOX releasing compared to reduction-insensitive cerasomes (RICs) in the presence of 10 mM of GSH. Under the same condition, the reduction sensibility of RRC was further proved by increased hydrodynamic diameter and destroying of integrity from DLS and SEM results. RRC showed non-toxic to human embryonic kidney 293 cells, indicating that this material has good biocompatibility. On the other hand, DOX/RRCs showed a resemble IC_{50} (half inhibitory concentration) value to that of free DOX to human hepatoma SMMC-7721 cells and breast cancer MCF-7 cells. IC_{50} values at 48 h were found to decrease in the following order: DOX/RIC > DOX/RRC > DOX. Taken together, the RRC developped in this study is of great potential to be utilized as a promising platform for intracellular anticancer drug delivery.

1. Introduction

The development of tumor-targeting drug delivery systems (DDSs), like liposomes [1–3], protein nanoparticles [4,5], inorganic nanoparticles [6,7] and polymeric micelles [8–10] has revived the therapeutic uses of numerous potent chemotherapeutics that are too toxic to be applied otherwise [11,12]. For instance, liposomes can protect their cargo by intrinsic shielding effect, hydrophilic drugs can be included in the inner water compartment of liposomes and lipophilic drugs can be incorporated into the liposome membrane [13]. With modifications of polyethylene glycol (PEG), the stealth liposome can evade the reticuloendothelial system (RES) of the body and get longer circulation time [14]. Nevertheless, major drawbacks of liposome-based drug carriers, including poor storage stability, premature leakage and the lack of tunable triggers for drug release, have limited their clinical applications [15]. Recently, a kind of liposome-like organic-inorganic biomimetic material named "cerasome" was developed based on organoalkoxysilane self-assembling [16–18]. The polyorganosiloxane surface endows cerasome a much higher stability than conventional liposomes [19]. Besides, cerasome exhibited a remarkable morphological resistance toward surfactant Triton X-100 (TX-100) and pH variation as compared to DMPC liposome that is only stable at pH 5.6. Moreover, the issue that traditional lipids in liposomes are easily oxidized was overcame within cerasome [20]. Furthermore, the problem of premature leakage of drugs was not observed in cerasome due to its high stability. However, high stability of cerasome make it hard to release its payload at the desired site of action, which limited its efficacy in cancer treatment. For instance, *in vitro* experiment showed that there was only 60% of drug (paclitaxel) release in cerasome

* Corresponding authors at: School of Biological Science & Medical Engineering, Southeast University, Nanjing 210096, China.
E-mail addresses: guning@seu.edu.cn (N. Gu), jimin@seu.edu.cn (M. Ji).

http://dx.doi.org/10.1016/j.colsurfb.2016.09.033
0927-7765/

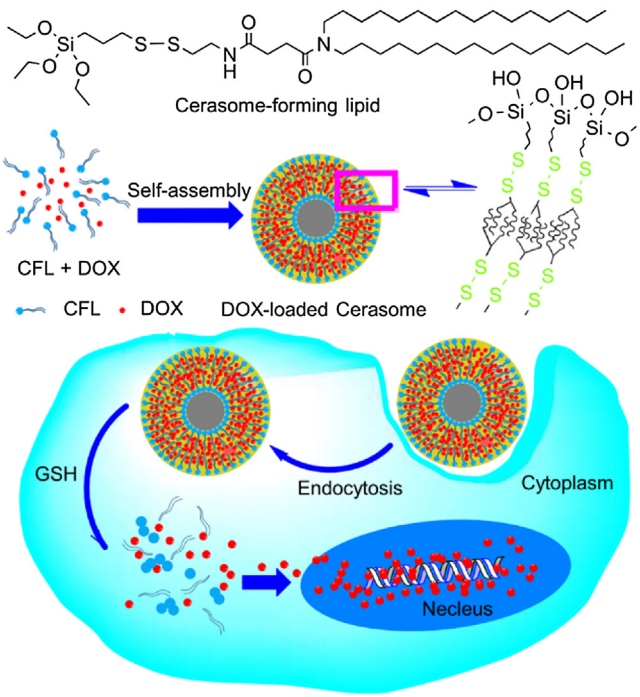

Fig. 1. Schematic illustration of the redox responsive cerasome for intracellular drug delivery.

even after 5 days [20]. Therefore, an ideal control over the drug release in cerasome is urgently essential.

Stimuli-responsive nanocarriers as good controlled drug delivery systems have attracted much attention in recent years [21]. Commonly used stimuli factors for the triggering of drug release include pH [22,23], temperature [24,25], redox [26–30], enzyme [31], light [32,33] and magnetism [34] *etc*. Glutathione (GSH) is the most abundant intracellular thiol-containing small molecule which involves in modulate disulfide cleavage reaction [35]. Due to the naturally occurring difference between the extra- and intra-cellular redox-environments, as well as elevated GSH level in tumor tissues (2–10 mM), disulfide bonds are increasingly being investigated as responsive linkers for DDSs [36–38].

In this study, a redox-responsive cerasome (RRC) drug delivery system was developed and evaluated. Of note, a novel organoalkoxysilane compound termed as cerasome-forming lipid (CFL) was designed and synthesized. It links triethoxysilyl head and hydrophobic alkyl double chain through a cleavable disulfide bond. As a precursor of an amphipathic molecule, CFL would form a bilayer vesicle called "cerasome" through sol-gel reaction (Fig. 1) [39]. It was demonstrated that this liposomal nanohybrid cerasome has higher morphological stability as compared to conventional liposome and it releases drugs in a redox responsive way, making RRC an ideal controlled release material. Besides, the synthesis of CFL is simple with low cost. The redox responsive release due to the breakage of disulfide at tumor-relevant glutathione (GSH) levels imparts cerasome an on-switch towards the intelligent drug delivery system. It would provide more strategies for developing anti-cancer drugs based on developing novel drug delivery systems.

2. Experimental section

2.1. Materials and instruments

Doxorubicin hydrochloride (DOX·HCl) was obtained from Beijing Huafeng United Technology Co. (Beijing, China). 1-Hexadecylamine, 1-bromohexadecane, succinic anhydride, 1-ethyl-3(3-(dimethylamino)propyl)carbodiimide·hydrochloride (EDC·HCl), 1-hydroxybenzotriazole (HOBt), triethylamine (TEA), *N*,*N*-diisopropylethylamine (DIPEA), Triton X-100 (TX-100) and glutathione (GSH) were purchased from Sinopharm Chemical Reagent Co., Ltd., China. 3-Mercaptopropyltriethoxysilane and 3-aminopropyltriethoxysilane were obtained from Sigma-Aldrich Co. (Shanghai, China), pyridine dithioethylamine hydrochloride was synthesized as previously described [40]. Solvents were purchased from local suppliers. THF was dried over sodium and freshly distilled before use.

^{1}H NMR and ^{13}C NMR data were recorded on AVANCE AV-300 NMR spectrometer (Bruker, Switzerland). HRMS spectra was obtained on 6500 Q-TOF mass analyser (Agilent, USA). Fluorescence spectra were recorded on F4600 spectrofluorometer (Hitachi, Japan). The surface morphology of cerasome samples was observed by Ultra Plus scanning electron microscopy (Zeiss, Germany). Size distribution and zeta potential were acquired using a Nano-ZS 90 Nanosizer (Malvern, UK).

2.2. Synthetic procedures

The CFL of RRC (**Lipid 2**) was synthesized by a four-step reaction as shown in Fig. 2. For comparison, a normal cerasome named reduction insensitive cerasome **(RIC)** was also prepared, its CFL (**Lipid 1**) without disulfide bond was synthesized according to literature procedure [41,42].

2.2.1. N,N-*Dihexadecylsuccinamic acid (1) [41,42]*

Dihexadecylamine was synthesized from hexadecylamine and bromohexadecane in ethanol at 40 °C in presence of potassium carbonate. The reaction mixture was filtered and washed with hot ethanol to get a white powder. Then the obtained dihexadecylamine (10.00 g, 21.47 mmol) and succinic anhydride (4.30 g, 43.00 mmol) were added to dry THF (100 mL) and dissolved upon heating. The solution was stirred for 24 h at room temperature. The solvent was evaporated in vacuum and the crude product was dissolved in dichloromethane (100 mL). The solution was then washed with 10% aqueous citric acid and saturated aqueous sodium chloride in this sequence. After removing residual water using phase separation filter paper, the solvent was evaporated in vacuum. Subsequent recrystallization from acetonitrile gave a white solid (9.12 g, 75.1%). ^{1}H NMR (300 MHz, $CDCl_3$) δ 3.31 (t, J = 7.4 Hz, 2H), 3.23 (t, J = 7.4 Hz, 2H), 2.68 (m, 4H), 1.55 (m, 4H), 1.26 (m, 52H), 0.88 (t, J = 6.2 Hz, 6H). ^{13}C NMR (75 MHz, $CDCl_3$) δ = 175.71, 171.84, 48.25, 46.61, 31.90, 30.21, 29.67, 29.63, 29.60, 29.55, 29.53, 29.36, 29.33, 28.83, 28.03, 27.65, 27.01, 26.89, 22.66, 14.06; Calcd. $[M + Na]^+$ $C_{36}H_{71}NO_3Na$, m/z = 588.5, found: $[M + Na]^+$ = 588.5.

2.2.2. N-*[N-[2-(2-Pyridinyldithio)]ethylsuccinamoyl]dihexadecylamine (2)*

To a solution of compound **1** (1.50 g, 2.65 mmol) in dry dichloromethane (30 mL) was added HOBt (0.43 g, 3.18 mmol), followed by EDCI (0.61 g, 3.18 mmol). After stirring for 30 min, *(S)*-2-pyridylthio cysteamine hydrochloride (0.59 g, 2.65 mmol) and TEA (0.44 mL, 3.18 mmol) were added to the solution, the mixture was stirred at 25 °C under nitrogen protection for 4 h. Then the mixture was washed with saturated brine, and dried over Na_2SO_4. The evaporation of the solvent gave the crude product that was purified with a silica gel column with ethyl acetate: hexane (2: 1) to furnish the colorless oil **2** (1.89 g, 97.1%). ^{1}H NMR (300 MHz, $CDCl_3$) δ 8.54 (d, J = 4.7 Hz, 1H), 7.59 (m, 2H), 7.34 (br. s, 1H), 7.13 (t, J = 5.7 Hz, 1H), 3.54 (d, J = 5.4 Hz, 2H), 3.36 – 3.13 (m, 4H), 2.92 (t, J = 6.0 Hz, 2H), 2.62 (dd, J = 20.3, 5.8 Hz, 4H), 1.63 – 1.43 (m, 4H), 1.26 (m, 52H), 0.88 (t, J = 6.5 Hz, 6H). ^{13}C NMR (75 MHz, $CDCl_3$) δ = 172.50, 171.09, 149.60, 136.69, 120.78, 120.27,

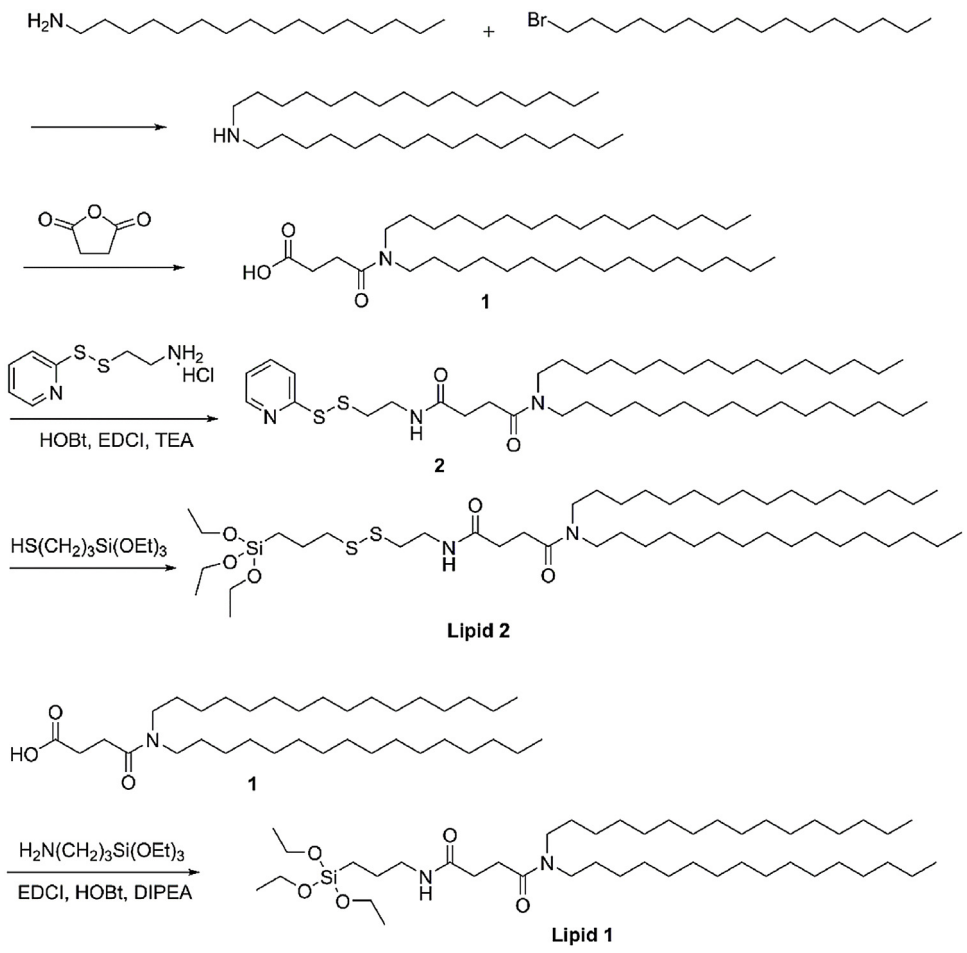

Fig. 2. Synthetic routes for cerasome-forming lipids.

47.80, 46.07, 38.46, 37.62, 31.61, 29.68–29.02, 28.66, 27.62, 26.82, 22.47, 13.89; Calcd. $[M+Na]^+$ $C_{43}H_{79}N_3O_2S_2Na$, m/z = 756.5, found: $[M+Na]^+$ = 756.5.

2.2.3. N-*[N-[2-[(3-Triethoxysilyl)propyl]dithio]ethylsuccinamoyl]dihexadecylamine (Lipid 2)*

To the solution of compound **2** (0.92 g, 1.25 mmol) in dry dichloromethane (30 mL) was added 3-mercaptopropyltriethoxysilane (0.60 mL, 2.50 mmol) and stirred at 25 °C for 48 h under nitrogen protection. Following the solvent evaporation, the residue was purified on a silica gel column with ethyl acetate: hexane (2: 5) to provide the pale yellow oil product **Lipid 2** (0.60 g, 55.7%). ^{1}H NMR (300 MHz, $CDCl_3$) δ 6.66 (br. s, 1H), 3.82 (q, J = 7.0 Hz, 6H), 3.55 (d, J = 6.0 Hz, 2H), 3.31 – 3.19 (m, 4H), 2.90 – 2.60 (m, 6H), 2.54 (m, 2H), 1.80 (dt, J = 15.3, 7.5 Hz, 2H), 1.51 (m, 4H), 1.43 – 1.11 (m, 61H), 0.88 (t, J = 6.4 Hz, 6H), 0.73 (t, J = 8.3 Hz, 2H). ^{13}C NMR (75 MHz, $CDCl_3$) δ = 172.74, 171.21, 58.35, 47.94, 46.26, 41.67, 38.20, 37.73, 31.86, 31.66, 29.63, 29.60, 29.55, 29.50, 29.39, 29.29, 28.88, 28.83, 27.76, 27.04, 26.90, 22.62, 22.57, 18.24, 14.03, 9.42; Calcd. $[M+Na]^+$ $C_{47}H_{96}N_2O_5S_2SiNa$, m/z = 883.64221, found: $[M+Na]^+$ = 883.64180.

2.2.4. N-*[N-(3-Triethoxysilyl)propylsuccinamoyl]dihexadecylamine (**Lipid 1**)*

HOBt (0.96 g, 7.12 mmol) and EDC·HCl (1.36 g, 7.12 mmol) was added with stirring at room temperature to a solution of *N*,*N*-dihexadecylsuccinamic acid (3.1 g, 5.48 mmol) in dry dichloromethane (30 mL). After 30 min of stirring, 3-aminopropyltriethoxysilane (1.6 g, 7.12 mmol) as well as DIPEA (0.6 g, 5.48 mmol) was added to the solution and the mixture was stirred for 4 h at room temperature before the reaction terminated. The solvent was evaporated in vacuum and column chromatography was carried out to finish the final purification. Impurities were eluted with dichloromethane/methanol 30: 1 and finally a colorless oil was obtained (2.5 g, 62%). ^{1}H NMR (300 MHz, $CDCl_3$) δ 6.37 (br. s., 1H), 3.81 (q, J = 7.0 Hz, 6H), 3.30 – 3.19 (m, 6H), 2.64 (t, J = 6.4 Hz, 2H), 2.51 (t, J = 6.2 Hz, 2H), 1.65 – 1.45 (m, 6H), 1.33-1.20 (m, 52H), 1.24 – 1.14 (m, 9H), 0.88 (t, J = 6.5 Hz, 6H), 0.62 (t, J = 8.4 Hz, 2H). ^{13}C NMR (75 MHz, $CDCl_3$) δ = 172.49, 171.34, 58.35, 47.96, 46.23, 41.92, 31.86, 31.80, 29.63, 29.59, 29.56, 29.50, 29.38, 29.29, 28.91, 27.75, 27.04, 26.90, 22.87, 22.62, 18.22, 14.02, 7.70; Calcd. $[M+Na]^+$ $C_{45}H_{92}N_2O_5SiNa$, m/z = 791.66677, found: $[M+Na]^+$ = 791.66897.

2.3. Preparation of cerasome and drug loaded cerasome

Both of the cerasomes were prepared by using a same ethanol injection method [43,44]. Briefly, the CFL was hydrolyzed in 1 mM of hydrochloric acid ethanol solution for 8 h, then the solution was reduced to dryness under reduced pressure on a rotary evaporator. After being redissolved in ethanol, it was injected to pure water (40 °C) with the volume ratio of 1: 9 (ethanol: water) under vigorous vortex. The prepared cerasome was stored at 40 °C for 24 h to allow the formation of surface network. Finally, ethanol was removed by dialysis using a dialysis bag with molecular weight cut-off (MWCO) 14,000 Da (Biosharp, USA).

For drug loading, firstly DOX·HCl (20 mg) was converted to free DOX base in the presence of TEA (DOX: TEA = 1: 1.2), after stirring for 30 min, it was freeze-dried and redissolved in DMSO (2 mL) after three times of washing with water. The DMSO solution of DOX was diluted with ethanol solution of hydrolyzed CFL and then injected into the pure water slowly. Unloaded drug was removed by centrifuge at 5000 rcf for 10 min. Residual solvents were removed by dialysis.

To determine the encapsulation efficiency of DOX in cerasome, 0.1 mL of as-prepared drug loaded cerasome was mixed with 0.9 mL of 90% ethanol solution with 0.075 M hydrochloric acid and allow to fully release of drug overnight. Then the absorption of DOX at 484 nm wavelength was recorded on an UV–vis spectrometer and the concentration was calculated according to the standard curve.

The encapsulation efficiency (EE) and drug loading capacity (DLC) were defined as follows [25,45]:

$$EE(\%) = (\text{mass of DOX in RRCs}/\text{mass of tota lDOX added}) \times 100\%$$

$$DLC(\%) = (\text{weight of DOX in RRCs}/\text{weight of DOX/RRCs}) \times 100\%$$

2.4. Stability of the RRCs

To investigate the storage stability of the RRCs, hydrodynamic diameters (D_{hy}) was determined by DLS at different time intervals. The resistance toward surfactant of the RRCs was also estimated by measuring the D_{hy} of cerasome with addition of TX-100 solution to vesicle suspension in varying proportions at room temperature. The D_{hy} of DPPC liposome was also investigated in parallel with control.

2.5. GSH-triggered release of DOX from RRCs

Sterilized dialysis bags with molecular weight cut-off (MWCO) 14,000 Da were used for drug release experiments. These dialysis bags were pretreated prior to use. Dialysis bags were fully immersed into 50% aqueous solution of ethanol and boiled 1 h, and then washed with plenty of water. To investigate the influence of pH value and redox potential on release of DOX, four different buffer were chosen: phosphate buffered saline (PBS, 10 mM, pH = 7.4), PBS (10 mM, pH = 7.4) with 10 mM of GSH, acetic buffer solutions (ABS, 10 mM, pH = 5.0) and ABS (10 mM, pH = 5.0) with 10 mM of GSH. The drug loaded cerasome samples (2 mL) were kept in the pretreated dialysis bags. The sealed dialysis bags were put into centrifugal tubes (50 mL) with 20 mL of release media. These tubes were packaged with aluminum foil to protect it from light and shaken at a speed of 100 rpm at 37 °C in an incubator shaker. At prescribed time intervals, 1 mL of the release media were taken out for measuring the released drug concentrations by the quantitative fluorescence spectrophotometric method (excitation wavelength: 484 nm, emission wavelength: 591 nm), and replaced with the original release media.

All drug release studies were carried out in triplicate. Normal cerasome loaded with DOX (DOX/RIC) was also tested as control at pH 5.0 and pH 7.4 respectively, in the presence of 10 mM GSH. The results were presented in terms of cumulative release as a function of time:

$$\text{Cumulative release}(\%) = (Mt/M_0) \times 100\%$$

where M_t is the amount of DOX released from cerasomes at time t and M_0 is the amount of DOX loaded in cerasome.

To assessment micellar stability of RRCs in response to GSH, sufficient GSH was added to RRCs suspension to achieve a 10 mM GSH reducing environment, the mixture was incubated at 37 °C in an incubator shaker and its hydrodynamic size distribution was determined at designated time intervals.

2.6. Cell culture

Human embryonic kidney 293 cell (HEK 293), human hepatoma SMMC-7721 cell and human breast cancer MCF-7 cell were provided by Cell Bank of Shanghai Institute of Cell Biology, Chinese Academy of Sciences. HEK 293 cells were maintained in Dulbecco's Modified Eagles' Medium (DMEM), supplemented with 10% fetal bovine serum (FBS) and 1% antibiotics (100 U mL^{-1} penicillin and 100 μg mL^{-1} streptomycin sulfate), SMCC-7721, MCF-7 cells were maintained in RPMI-1640 supplemented 10% FBS and 1% antibiotics. All cells were cultured in a humidified 5% CO_2 atmosphere at 37 °C. Medium was replaced in every other day of subcultures.

2.7. Cell viability assay

The CCK-8 assays were conducted to assess the biocompatibility of cerasome to normal tissue cells (HEK 293) as well as the antitumor activity of DOX-loaded cerasomes to SMCC-7721 and MCF-7 cells. Briefly, 5000 cells per well were seeded in 96-well plates in 100 μL of complete culture medium (containing 10% fetal bovine serum) and incubated at 37 °C in a CO_2 incubator for 24 h. Then the volume in each well was replaced with 100 μL of blank or DOX loaded cerasome treatment medium. Varied DOX concentrations 0.001, 0.01, 0.1, 1, 3 μM were tested with free DOX as positive control. At the end of the incubation period, 10 μL of CCK-8 reagent (Beyotime, Shanghai, China) was added to the cells and further incubated for 4 h. Afterward the 96-well plate was analyzed at a 450 nm wavelength in an Infinite 200 PRO plate reader (Tecan, Switzerland) to determine cell viability. Media without test material was used as control.

3. Results and discussion

3.1. Preparation and characterization

A disulfide bond was creatively introduced to the precursor of existing cerasome [16]. Dihexadecylamine in reaction with succinic anhydride to give compound **1** which reacted with *(S)*-2-pyridylthio cysteamine hydrochloride giving compound **2**. **Lipid 2** was synthesized from compound **2** via a disulfide exchange reaction. **Lipid 1**, the CFL of RIC, was also synthesized as a control. The target molecules were characterized by ^{1}H NMR, ^{13}C NMR and mass spectra (see Supporting information). In order to fabricate cerasomes, the CFL was hydrolyzed in acidic ethanol to produce an amphipathic molecule which has a hydrophilic head consisting of silanol groups. Ethanol injection method gave a transparent cerasome suspension, doxorubicin, a widely used anticancer drug, was loaded as a model drug (Fig. S11A). Preparation method was optimized in aspects of hydrolysis condition of CFL, water temperature and molar ratio of CFL to drug. Characterization of cerasome samples including size, zeta potential, EE (%) and DLC (%) were shown in Table 1. Scan electron microscopy (SEM) image (Fig. 3B) showed good monodispersity and uniform size of the RRCs. The average hydrodynamic diameters (D_{hy}) and zeta potential were determined to be 177.8 nm (PDI = 0.159) (Fig. 3A) and −33.5 mV for the empty RRCs, 185.4 nm (PDI = 0.172) and −25.6 mV for DOX/RRCs (Table 1). There was no obvious difference in size, zeta potential and EE (%) between RIC and RRC. The RRCs appeared to be slightly larger when analysed by dynamic light scattering (DLS) due to the presence of a hydration layer around the vesicles in aqueous media [46]. The empty RRCs possessed a high negative zeta potential, most likely due to the presence of silanol groups on the outer face of cerasomes, indicating that the triethoxysilyl moieties of the CFL were

Table 1
Characterization of blank and DOX-loaded cerasomes (theoretical DLC = 3.2 wt%).

Sample	Blank cerasome			DOX-loaded cerasome			EE(%)[b]	DLC(wt%)[b]
	D_{hy} (nm)[a]	PDI[a]	Zeta potential (mV)[a]	D_{hy} (nm)[a]	PDI[a]	Zeta potential (mV)[a]		
RRC	177.8	0.159	−33.5	185.4	0.172	−25.6	74.3	2.4
RIC	174.6	0.127	−35.6	180.8	0.104	−26.4	75.7	2.5

[a] Determined by dynamic light scattering (DLS), n = 3.
[b] Determined by UV–vis absorption spectrum, n = 3.

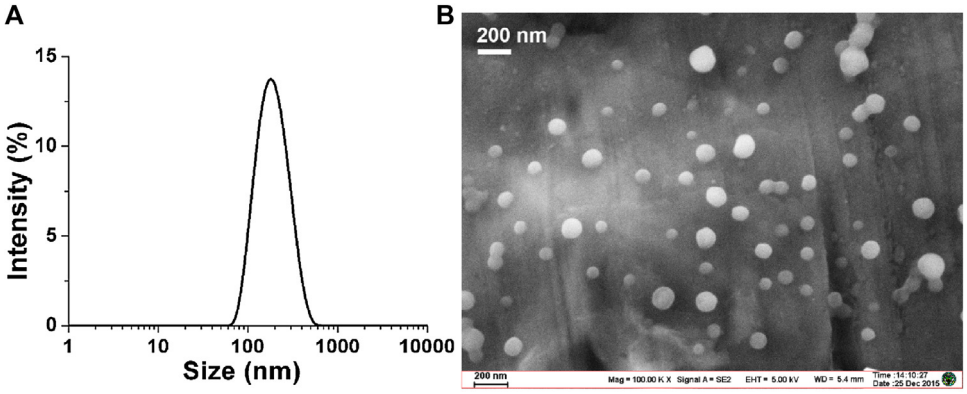

Fig. 3. (A) Hydrodynamic diameter distribution of RRCs in water (B) SEM micrograph of RRCs with scale bar of 200 nm.

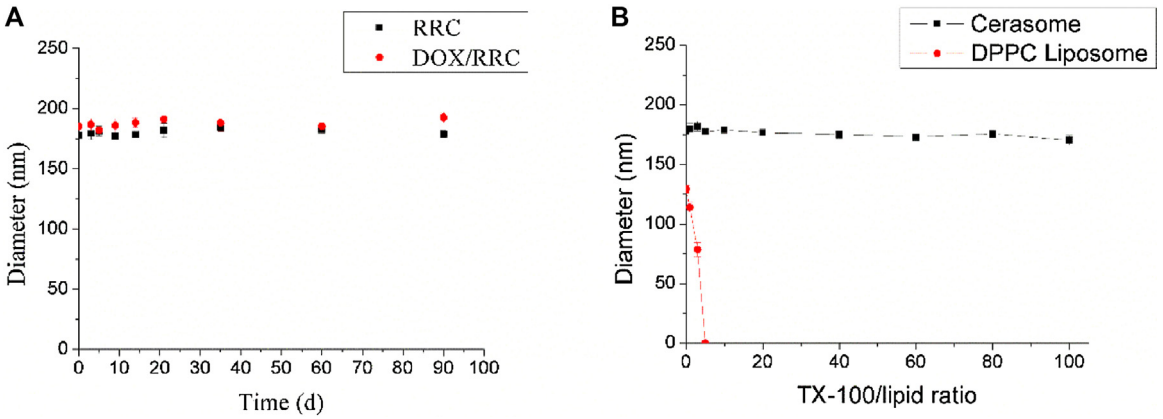

Fig. 4. Hydrodynamic diameter (D_{hy}) of cerasomes during storage (A) and upon the addition of Triton X-100 (B) (error bar denotes standard deviation, n = 3).

hydrolyzed and negatively charged, and that the hydrolyzed triethoxysilyl groups were partially polymerized [47], which imparts the cerasome a good colloidal stability.

Hydrophobic DOX was believed to present in the hydrophobic domain of the lipid bilayer [12,13]. The fluorescence quenching of DOX loaded in cerasomes was observed by fluorescence recovery after being released from RRCs (Fig. S11B). DOX was loaded into RRCs at a theoretical drug loading content (DLC) of 3.2 wt%. The results showed an encapsulation efficiency (EE) of 74.3% (20:1 lipid-to-drug ratio) for RRCs, which led to a decent DOX loading of 2.4 wt% (Table 1). The loading of DOX had little influence on D_{hy} of cerasomes.

3.2. Stability of cerasome

The oxidation and hydrolysis of lipid, the aggregation and fusion of vesicle structure, especially the resulting drug leakage are of challenging to the *in vivo* application of liposome [48]. In the case of cerasome, its specific characters such as high zeta potential and stable silica-like surface with siloxane framework will give cerasome an enhanced resistance to aggregation and thus improved morphological stability. In order to provide further evidences, long storage and surfactants resistance experiments were conducted. There was no significant change in sizes during 90 days' storage (Fig. 4A). The morphological stability of cerasome against membrane solubilizing agent was also evaluated, in comparison with DPPC liposome, there was no change in the size of RRCs upon the addition of 100 equiv. of TX-100, but liposomes totally dissolved when 5 equiv. of TX-100 was added to liposome suspension, indicating that cerasomes had remarkably high morphological stability than liposomes (Fig. 4B). All these results proved that both the novel cerasome and literature reported cerasome are comparable in stability [20]. Usually, the polysiloxane network grew with increasing incubation time and as-prepared cerasome requires more than 24 h to form polysiloxane network on the surface. Surfactant solubilization is a typical method to evaluate morphological stability of liposomes in aqueous media. The surfactant can insert into lipid bilayer and destroy the stability of self-assembly structure. But on the surface

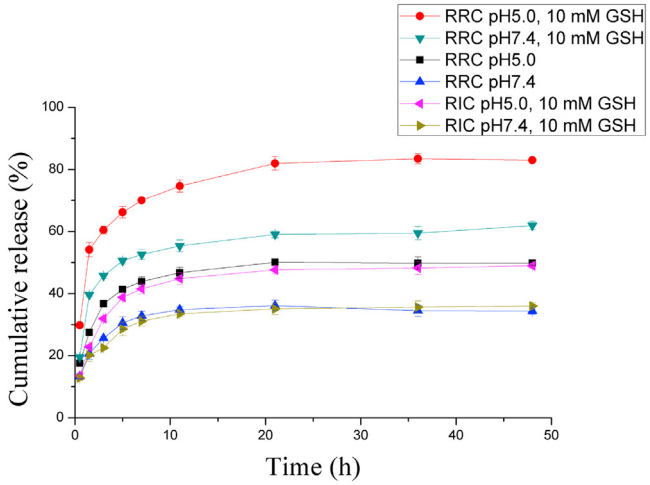

Fig. 5. Redox-triggered release of DOX from RRCs (at pH 7.4 and 5.0, 10 mM GSH, error bar denotes standard deviation, n = 3), the RIC was used as a reduction insensitive control.

of stable cerasome, the polysiloxane network limited the mobility of membrane, which make it ineffective for the surfactant to break the cerasome. To determine EE% and DL%, as-prepared cerasome without complete polysiloxane network was used. Treatment with acid alcohol solution allows as-prepared cerasome to release loaded DOX totally. Hence, stability during long time storage, as well as the morphological stability against fusion and precipitation, made cerasome an effective controlled-release carrier for anticancer drugs without premature leakage.

3.3. In vitro *drug release*

In vitro release of DOX from RRCs was investigated at pH 5.0 and 7.4 respectively for pH dependent solubility of DOX. It was performed under redox stimulation using dissolution medium with or without GSH at each pH value. Cumulative release (%) values of DOX in four dissolution media were measured as well. For DOX/RRCs, the results (Fig. 5) showed that only 34.4% of DOX was released within 48 h at physiological pH (7.4). DOX release was significantly accelerated at pH 5.0 by 61.8% of DOX released within 48 h under same condition, meaning that 38.2% of drug still remains in the vesicles. Notably, DOX release was boosted under reductive condition (10 mM GSH, pH 7.4), in which 79.8% of drug was released within 48 h. The fastest and most complete drug release was observed at pH 5.0 with the presence of 10 mM GSH where in 82.0% of DOX was released in 21 h. In comparison, normal cerasome have no response to GSH, DOX release in RIC under reductive condition was similar to the situation of RRC under non-reductive condition. Therefore, different with the traditional cerasome, DOX encapsulated in RRC was released in a redox responsive manner. We propose that the acidic and reductive environment of tumor would contribute to the local release of DOX from RRCs, making it a suitable delivery system for cancer chemotherapy. In addition, GSH-induced disassembly of RRCs was evaluated through DLS and SEM. Time dependent aggregate size of RRCs was monitored upon exposure to 10 mM GSH (Fig. 6A), SEM observation revealed the damage of structural integrity (Fig. 6B). These results revealed why drugs loaded in the RRCs released in a redox responsive way. The high negative surface charge and siloxane network on the surface of cerasome endow cerasome high stability which enhanced its ability to adapt acid, alkali and surfactant environments. Under reductive condition, for example, with the presence of GSH, the lipid bilayer structure could be destroyed after the breakage of disulfide bond, leading to the release of cargo, otherwise polymerization reaction among silanols on each fragment may occur, which can result in aggregation of fragments. Due to its remarkable colloidal stability and morphological stability, RRC can protect its cargo from premature leakage; on the other hand, the response to reductive molecules such as GSH in cytoplasm components made it an intelligent redox-responsive carrier for delivery of anticancer drugs.

Table 2
IC_{50} values of DOX and DOX loaded cerasomes to tumor cells (μM).

Cell type	DOX	RIC/DOX	RRC/DOX
SMCC-7721	0.32	2.24	0.58
MCF-7	1.10	3.84	1.70

3.4. *Cytotoxicity evaluation*

Biocompatibility assessments of cerasomes were conducted by determining the cytotoxicity to human embryonic kidney 293 cells. The results demonstrated that cell viability of HEK 293 was not significantly affected upon exposure to both cerasomes. After treatment with RIC or RRC, cell viabilities were more than 91.2% at 24 h (Fig. 7A) and over 85.5% at 48 h (Fig. 7B) at various concentrations, the highest treatment concentration was 0.5 mg mL^{-1}. These data indicated that both RIC and RRC have good biocompatibility.

The antitumor activity of DOX/RICs and DOX/RRCs were evaluated by determining the cytotoxicities using human hepatoma SMMC-7721 cells and human breast cancer MCF-7 cells, with free DOX as control. The results revealed that empty cerasomes (both RIC and RRC) were practically non-toxic (cell viability ≥ 88.3% at 48 h) to both SMCC-7721 and MCF-7 cell under the highest treatment (Fig. 7C, 7D). Drug loaded cerasomes, however, displayed significant antitumor activity toward SMCC-7721 and MCF-7 cell during 48 h (Fig. 7C,D) incubation. For both tumor cells, the IC_{50} (half inhibitory concentration) values at 48 h from highest to lowest were: DOX/RIC > DOX/RRC > DOX (Table 2). Furthermore, DOX/RRC was found as active as free drug and showed a similar IC_{50} value to that of free DOX, while DOX/RRCs showed higher antitumor efficiency than DOX/RICs, this should be attributed to quickly intracellular release of DOX from RRCs under stimulation of GSH in cytoplasm of cancer cells.

4. Conclusions

In this study, a novel redox-responsive liposomal nanohybrid cerasome was developed based on organosilicone precursor. The cerasome-forming lipid (CFL) that comprise a cleavable disulfide bond as connector unit of the triethoxysilyl head and the hydrophobic alkyl double chain was creatively designed and synthesized, which assembled into lipid bilayer vesicles in aqueous solution by a sol-gel process. This biomimetic material possessed remarkably high morphological stability due to its crosslinked siloxane network on the surface. Using doxorubicin as model drug, RRC was proved to release the payload in response to chemically triggered reduction. Non-toxic to Heck 293 cells indicated good biocompatibility of RRCs towards normal cells while DOX/RRCs showed effective cytotoxicity against tumor cells. The RRC as drug carrier has two advantages: first, low premature leakage due to its extremely stable silicate surface; second, intracellular controllable release that can be triggered by local reducing environment in the intracellular compartment of cancer cells. Given the feature of high stability and flexible control release within RRC developed in this study, it will make a great contribution to the development of cancer drug delivery. In the future, more extensive study on the clinical application is worth being performed to confirm its role as a promising candidate for ideal drug delivery system.

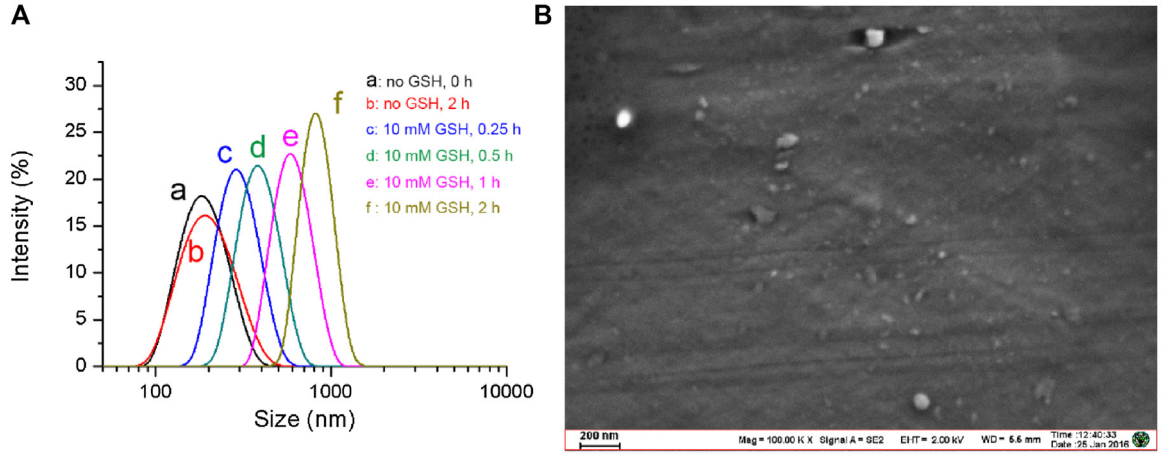

Fig. 6. GSH induced disassembly of RRCs determined by DLS and SEM (A) Time-dependent changes in D_{hy} of RRCs upon exposure to 10 mM GSH at 37 °C as determined by DLS; (B) SEM micrograph of RRCs after incubation with 10 mM GSH solution.

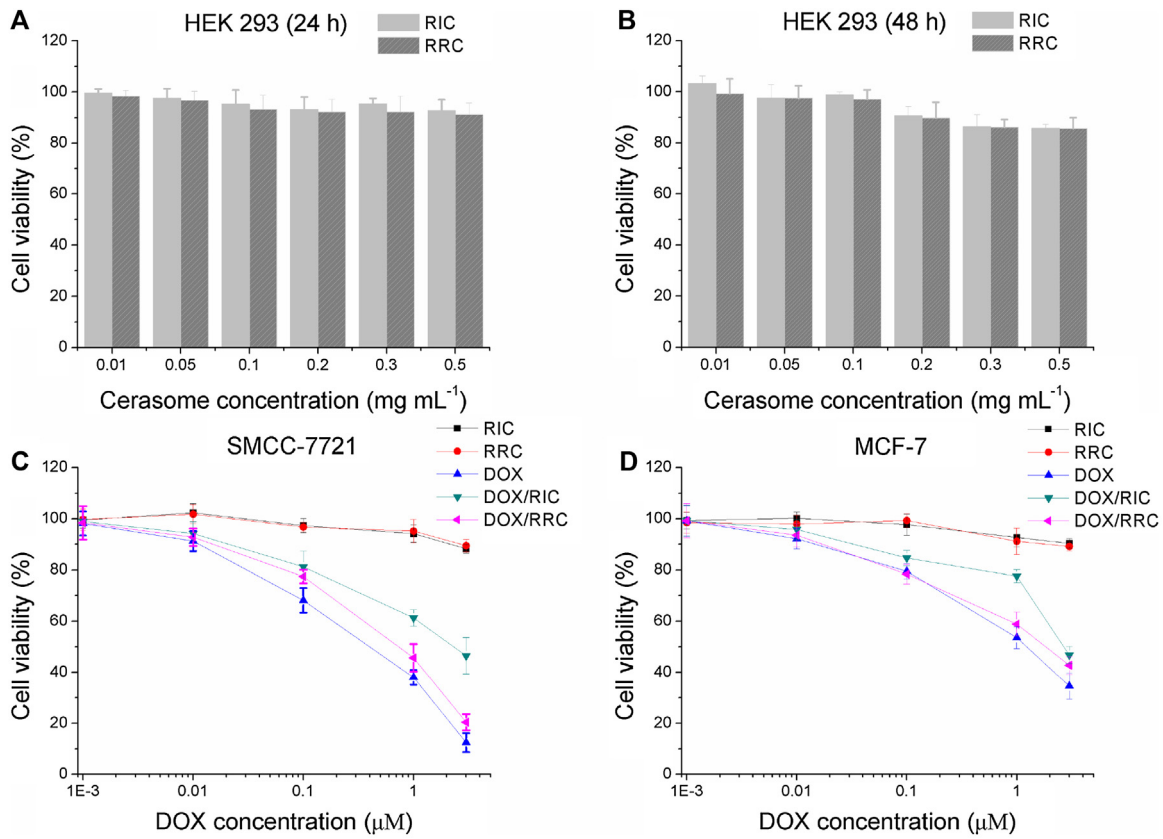

Fig. 7. Biocompatibility assessment and antitumor efficiency evaluation by CCK-8 assay: The inhibition of empty cerasomes towards HEK 293 cell at (A) 24 h and (B) 48 h, DOX or DOX loaed cerasome towards (C) SMCC-7721 cell and (D) MCF-7 cell at 48 h (error bar denotes standard deviation, n = 3).

Acknowledgements

This research was financially supported by National High-tech Research and Development Project (863 Project, 2013AA032205), National Key Basic Research Program of China (973 Program, 2013CB933904), Industry Project of Jiangsu Science-technology Support Plan(BE2013840), Science and Technology Development Program of Suzhou (ZXY201412), National basic Research Program of China (2013CB934400).

Appendix A. Supplementary data

Supplementary data associated with this article can be found, in the online version, at http://dx.doi.org/10.1016/j.colsurfb.2016.09.033.

References

[1] D.D. Lasic, D. Needham, The stealth liposome: a prototypical biomaterial, Chem. Rev. 95 (1995) 2601–2628.

[2] D.D. Lasic, D. Papahadjopoulos, Liposomes and biopolymers in drug and gene delivery, Curr. Opin. Solid State Mater. Sci. 1 (1996) 392–400.
[3] M. Silindir, S. Erdogan, A.Y. Ozer, S. Maia, Liposomes and their applications in molecular imaging, J. Drug Target. 20 (2012) 401–415.
[4] A. Makino, S. Kimura, Preparation of peptide- and protein-based molecular assemblies and their utilizations as nanocarriers for tumor imaging, React. Funct. Polym. 71 (2011) 272–279.
[5] M. Jahanshahi, Z. Babaei, Protein nanoparticle: a unique system as drug delivery vehicles, Afr. J. Biotechnol. 7 (2008) 4926–4934.
[6] T. Murakami, K. Tsuchida, Recent advances in inorganic nanoparticle-based drug delivery systems, Mini-Rev. Med. Chem. 8 (2008) 175–183.
[7] Y. Chen, H. Chen, J. Shi, Inorganic nanoparticle-based drug codelivery nanosystems to overcome the multidrug resistance of cancer cells, Mol. Pharm. 11 (2014) 2495–2510.
[8] M. Elsabahy, G.S. Heo, S.M. Lim, G. Sun, K.L. Wooley, Polymeric nanostructures for imaging and therapy, Chem. Rev. 115 (2015) 10967–11011.
[9] S. De Koker, L.J. De Cock, P. Rivera-Gil, W.J. Parak, R. Auzely Velty, C. Vervaet, J.P. Remon, J. Grooten, B.G. De Geest, Polymeric multilayer capsules delivering biotherapeutics, Adv. Drug Deliv. Rev. 63 (2011) 748–761.
[10] Y. Li, D. Maciel, J. Rodrigues, X. Shi, H. Tomas, Biodegradable polymer nanogels for drug/nucleic acid delivery, Chem. Rev. 115 (2015) 8564–8608.
[11] C. Deng, Y. Jiang, R. Cheng, F. Meng, Z. Zhong, Biodegradable polymeric micelles for targeted and controlled anticancer drug delivery: promises, progress and prospects, Nano Today 7 (2012) 467–480.
[12] Y. Min, J.M. Caster, M.J. Eblan, A.Z. Wang, Clinical translation of nanomedicine, Chem. Rev. (2015) 11147–11190.
[13] V.P. Torchilin, Recent advances with liposomes as pharmaceutical carriers, Nat. Rev. Drug Discov. 4 (2005) 145–160.
[14] D.D. Lasic, D. Needham, The stealth liposome: a prototypical biomaterial, Chem. Rev. 95 (1995) 2601–2628.
[15] S.M. Lee, H. Chen, C.M. Dettmer, T.V. O'Halloran, S.T. Nguyen, Polymer-caged lipsomes: a pH-responsive delivery system with high stability, J. Am. Chem. Soc. 129 (2007) 15096–15097.
[16] Z. Cao, X. Yue, Y. Jin, X. Wu, Z. Dai, Modulation of release of paclitaxel from composite cerasomes, Colloid Surf. B-Biointerfaces 98 (2012) 97–104.
[17] Z. Dai, W. Tian, X. Yue, Z. Zheng, J. Qi, N. Tamai, J.-I. Kikuchi, Efficient fluorescence resonance energy transfer in highly stable liposomal nanohybrid cerasome, Chem. Commun. (2009) 2032–2034.
[18] K. Katagiri, K. Ariga, J.-i. Kikuchi, Preparation of organic-inorganic hybrid vesicle cerasome derived from artificial lipid with alkoxysilyl head, Chem. Lett. 30 (1999) 661–662.
[19] Y. Wang, B. Wang, H. Liao, X. Song, H. Wu, H. Wang, H. Shen, M. Tan, Liposomal nanohybrid cerasomes for mitochondria-targeted drug delivery, J. Mater. Chem. B 3 (2015) 7291–7299.
[20] Z. Cao, Y. Ma, X. Yue, S. Li, Z. Dai, J. Kikuchi, Stabilized liposomal nanohybrid cerasomes for drug delivery applications, Chem. Commun. 46 (2010) 5265–5267.
[21] C.A. Lorenzo, A. Concheiro (Eds.), Smart Materials for Drug Delivery, vol. 1, RSC, UK, 2013 (Chapter 1).
[22] R. Liu, Y. Zhang, X. Zhao, A. Agarwal, L.J. Mueller, P. Feng, pH-responsive nanogated ensemble based on gold-capped mesoporous silica through an acid-labile acetal linker, J. Am. Chem. Soc. 132 (2010) 1500–1501.
[23] A. Popat, J. Liu, G.Q. Lu, S.Z. Qiao, A pH-responsive drug delivery system based on chitosan coated mesoporous silica nanoparticles, J. Mater. Chem. 22 (2012) 11173–11178.
[24] B. Zhang, J. Chen, Y. Lu, J. Qi, W. Wu, Liposomes interiorly thickened with thermosensitive nanogels as novel drug delivery systems, Int. J. Pharm. 455 (2013) 276–284.
[25] Y. Wang, G. Wu, X. Li, J. Chen, Y. Wang, J. Ma, Temperature-triggered redox-degradable poly(ether urethane) nanoparticles for controlled drug delivery, J. Mater. Chem. 22 (2012) 25217–25226.
[26] H. Zhang, K. Wang, P. Zhang, W. He, A. Song, Y. Luan, Redox-sensitive micelles assembled from amphiphilic mPEG-PCL-SS-DTX conjugates for the delivery of docetaxel, Colloid Surf. B-Biointerfaces 142 (2016) 89–97.
[27] N. Song, W. Liu, Q. Tu, R. Liu, Y. Zhang, J. Wang, Preparation and in vitro properties of redox-responsive polymeric nanoparticles for paclitaxel delivery, Colloid Surf. B-Biointerfaces 87 (2011) 454–463.
[28] Z.-Y. Li, J.-J. Hu, Q. Xu, S. Chen, H.-Z. Jia, Y.-X. Sun, R.-X. Zhuo, X.-Z. Zhang, A redox-responsive drug delivery system based on RGD containing peptide-capped mesoporous silica nanoparticles, J. Mater. Chem. B 3 (2015) 39–44.
[29] H. Ren, Y. Wu, N. Ma, H. Xu, X. Zhang, Side-chain selenium-containing amphiphilic block copolymers: redox-controlled self-assembly and disassembly, Soft Matter 8 (2012) 1460–1466.
[30] H. Sun, B. Guo, R. Cheng, F. Meng, H. Liu, Z. Zhong, Biodegradable micelles with sheddable poly(ethylene glycol) shells for triggered intracellular release of doxorubicin, Biomaterials 30 (2009) 6358–6366.
[31] K. Patel, S. Angelos, W.R. Dichtel, A. Coskun, Y.W. Yang, J.I. Zink, J.F. Stoddart, Enzyme-responsive snap-top covered silica nanocontainers, J. Am. Chem. Soc. 130 (2008) 2382–2383.
[32] V. Voliani, F. Ricci, G. Signore, R. Nifosi, S. Luin, F. Beltram, Multiphoton molecular photorelease in click-chemistry-functionalized gold nanoparticles, Small 7 (2011) 3271–3275.
[33] Z.X. Zhang, D. Balogh, F. Wang, R. Tel-Vered, N. Levy, S.Y. Sung, R. Nechushtai, I. Willner, Light-induced and redox-triggered uptake and release of substrates to and from mesoporous SiO_2 nanoparticles, J. Mater. Chem. B 1 (2013) 3159–3166.
[34] C.R. Thomas, D.P. Ferris, J.H. Lee, E. Choi, M.H. Cho, E.S. Kim, J.F. Stoddart, J.S. Shin, J. Cheon, J.I. Zink, Noninvasive remote-controlled release of drug molecules in vitro using magnetic actuation of mechanized nanoparticles, J. Am. Chem. Soc. 132 (2010) 10623–10625.
[35] M.H. Lee, Z. Yang, C.W. Lim, Y.H. Lee, S. Dongbang, C. Kang, J.S. Kim, Disulfide-cleavage-triggered chemosensors and their biological applications, Chem. Rev. 113 (2013) 5071–5109.
[36] Z.B. Zheng, G. Zhu, H. Tak, E. Joseph, J.L. Eiseman, D.J. Creighton, N-(2-hydroxypropyl)methacrylamide copolymers of a glutathione (GSH)-activated glyoxalase i inhibitor and DNA alkylating agent: synthesis, reaction kinetics with GSH, and in vitro antitumor activities, Bioconjug. Chem. 16 (2005) 598–607.
[37] L. Brulisauer, M.A. Gauthier, J.C. Leroux, Disulfide-containing parenteral delivery systems and their redox-biological fate, J. Control. Release 195 (2014) 147–154.
[38] H. Han, H. Wang, Y. Chen, Z. Li, Y. Wang, Q. Jin, J. Ji, Theranostic reduction-sensitive gemcitabine prodrug micelles for near-infrared imaging and pancreatic cancer therapy, Nanoscale 8 (2015) 283–291.
[39] K. Katagiri, M. Hashizume, K. Ariga, T. Terashima, J.-i. Kikuchi, Preparation and characterization of a novel organic-inorganic nanohybrid cerasome formed with a liposomal membrane and silicate surface, Chem.-Eur. J. 13 (2007) 5272–5281.
[40] G.T. Zugates, D.G. Anderson, S.R. Little, I.E. Lawhorn, R. Langer, Synthesis of poly(beta-amino ester)s with thiol-reactive side chains for DNA delivery, J. Am. Chem. Soc. 128 (2006) 12726–12734.
[41] L.S. Li, G.X. Zhou, J. Cai, J.Q. Chen, P. Wang, T.Z. Zhang, M. Ji, N. Gu, Preparation and characterization of a novel nanocomposite: silver nanoparticles decorated cerasome, J. Sol-Gel. Sci. Technol. 69 (2014) 199–206.
[42] K. Katagiri, M. Hashizume, K. Ariga, T. Terashima, J.-i. Kikuchi, Preparation and characterization of a novel organic-inorganic nanohybrid cerasome formed with a liposomal membrane and silicate surface, Chem. Eur. J. 13 (2007) 5272–5281.
[43] M. Hashizume, I. Saeki, M. Otsuki, J.-I. Kikuchi, Incorporation of lipid domains in Cerasome, a morphologically-stable organic-inorganic vesicular nanohybrid, J. Sol-Gel. Sci. Technol. 40 (2006) 227–232.
[44] M. Hashizume, H. Horii, J.-i. Kikuchi, M. Kamitakahara, C. Ohtsuki, M. Tanihara, Effects of surface carboxylic acid groups of cerasomes, morphologically stable vesicles having a silica surface, on biomimetic deposition of hydroxyapatite in body fluid conditions, J. Mater. Sci. Mater. Med. 21 (2010) 11–19.
[45] L. Yuan, Q. Tang, D. Yang, J.Z. Zhang, F. Zhang, J. Hu, Preparation of pH-responsive mesoporous silica nanoparticles and their application in controlled drug delivery, J. Phys. Chem. C 115 (2011) 9926–9932.
[46] A. Wagh, F. Jyoti, S. Mallik, S. Qian, E. Leclerc, B. Law, Polymeric nanoparticles with sequential and multiple FRET cascade mechanisms for multicolor and multiplexed imaging, Small 9 (2013) 2129–2139.
[47] Y. Jin, X. Yue, Q. Zhang, X. Wu, Z. Cao, Z. Dai, Cerasomal doxorubicin with long-term storage stability and controllable sustained release, Acta Biomater. 8 (2012) 3372–3380.
[48] B. Mandal, H. Bhattacharjee, N. Mittal, H. Sah, P. Balabathula, L.a. Thoma, G.C. Wood, Core-shell-type lipid-polymer hybrid nanoparticles as a drug delivery platform, Nanomed.-Nanotechnol, Biol. Med. 9 (2012) 474–491.